

Signal Amplification by Changing Counterions in Conjugated Polyelectrolyte-Based FRET DNA Detection

Mijeong Kang,[†] Okhil Kumar Nag,[†] Rati Ranjan Nayak,[†] Sungu Hwang,[†]
Hongseok Suh,[‡] and Han Young Woo^{*,†}

Department of Nanofusion Technology (BK21), Pusan National University, Miryang 627-706, South Korea, and Department of Chemistry, Pusan National University, Busan 609-735, South Korea

Received November 25, 2008; Revised Manuscript Received January 15, 2009

ABSTRACT: Two types of cationic polyfluorene copolymers (**FHQ**, **FPQ**) with a same π -conjugated structure but different counterions (bromide (**BR**), tetraphenylborate (**PB**)) were synthesized and studied as a fluorescence resonance energy transfer (FRET) donor to fluorescein-labeled DNA (ssDNA-Fl). The counterions accompanying the polymer chain for charge compensation are expected to perturb complexation with DNA and modify the fine-structure of D/A complex on molecular scale, which may influence the competition between the desirable FRET and energy-wasting charge transfer quenching. The PL quenching constant of ssDNA-Fl by Stern–Volmer plot was significantly reduced in the presence of the polymers with tetraphenylborate ($4.3 \times 10^6 \text{ M}^{-1}$ for **FHQ-BR** vs $2.2 \times 10^6 \text{ M}^{-1}$ for **FHQ-PB**, $2.8 \times 10^6 \text{ M}^{-1}$ for **FPQ-BR** vs $1.3 \times 10^6 \text{ M}^{-1}$ for **FPQ-PB**). The resulting FRET-induced signal was amplified 2 to 8.6 times by exchanging bromide with tetraphenylborate as a counterion, suggesting a simple way for kinetic control of energy transfer to maximize signal amplification in conjugated polymer-based FRET biosensors.

1. Introduction

Water-soluble conjugated polyelectrolytes (CPs) have an interesting structure characterized by a π -conjugated main backbone and ionic side groups.^{1,2} They have the useful optical- and/or electronic properties of organic semiconductors as well as solubility in highly polar media such as water. Various CPs have been reported as an optical platform for chemical- and biological assays.^{2,3} Among them, cationic CPs (CCPs) with terminal quaternary ammonium groups have found interesting applications in optical DNA detection using colorimetric change⁴ or fluorescence resonance energy transfer (FRET) mechanisms.⁵ Electrostatic complexation between CCPs and negatively charged DNA either induces a conformational change in the conjugated backbone or can be coordinated to give rise to an efficient FRET to signal a sequence-specific target DNA.

The latter scheme proposed by Bazan benefits from the light-harvesting (or antenna-like) properties of water-soluble CCPs to achieve sensory signal amplification.⁵ Electrostatic interactions between the CCPs and fluorophore-labeled peptide nucleic acid (PNA) or DNA hybridized with the target DNA bring them into close proximity by forming an electrostatic complex, which satisfies the FRET distance condition. Several studies have focused on optimizing the FRET process to maximize the signal amplification provided by CPs.^{5–8} These efforts highlight the importance of matching the energy levels and controlling the intermolecular distance between the donor–(D–) acceptor (A) pairs to minimize the energy-wasting photoinduced charge transfer (PCT) quenching which competes with the desirable FRET. Recent studies have succeeded in decreasing PCT substantially, and have observed enhanced FRET-induced signal by modulating the intermolecular D–A distance (r_{D-A}) by attaching molecular spacers on the CCP chain,⁶ varying the chain length of the alkyl substituents on the polymer backbone⁷ or using buffer/organic solvent mixtures in which the electrostatic complexation of CCP and DNA is modified.⁸ Both FRET

and PCT are very sensitive to the intermolecular D–A distance: PCT is essentially a contact process described by an exponential distance dependence and the FRET rate (k_{FRET}) is proportional to r_{D-A}^{-6} .⁹ Therefore, the competition between them is possibly controlled by the D–A distance modulation on the molecular scale. Another approach was also reported by modifying the HOMO and LUMO energy levels to decrease the PCT energetically between the CCPs and the probe dye.¹⁰ However, both kinetic and thermodynamic controls have difficulty in that they require complicated chemical synthesis to modify the molecular structures. Therefore, there is a need for a simple and general way of controlling PCT and FRET. The molecular structure of the CCP must play an important role in determining the overall structure of the D/A pairs, the distance between the optically active backbone and the probe dye, and the degree to which FRET or PCT takes place.⁶ These are poorly understood, and require fine-control in order to optimize CPs-based DNA detection.

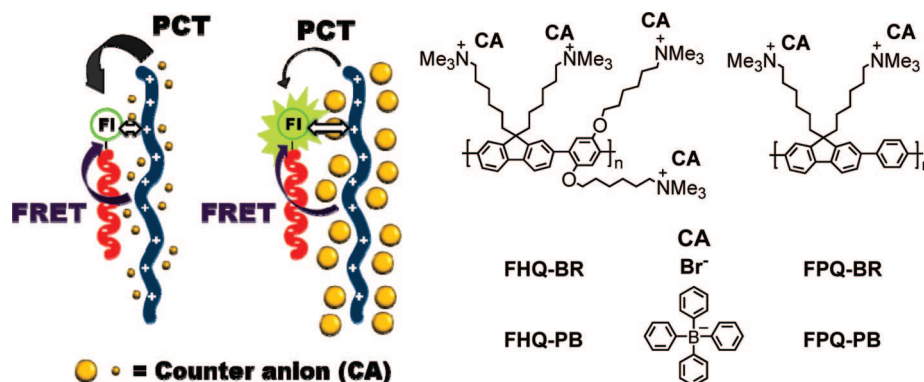
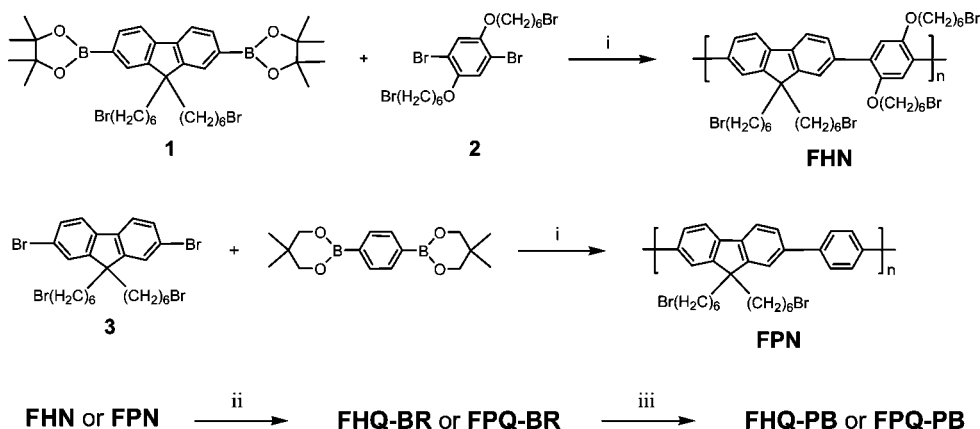
In this contribution, we report the molecular design and FRET-related photophysical properties of two water-soluble CCPs (as a FRET donor) with two different counterions (bromide and tetraphenylborate), poly(9,9'-bis(6-*N,N,N*-trimethylammoniumhexyl)fluorene-*alt*-1,4-(2,5-bis(6-*N,N,N*-trimethylammoniumhexyloxy))phenylene) containing bromide (**FHQ-BR**) and tetraphenylborate (**FHQ-PB**), and poly(9,9'-bis(6-*N,N,N*-trimethylammoniumhexyl)fluorene-*alt*-phenylene) with bromide (**FPQ-BR**) and tetraphenylborate (**FPQ-PB**) (Scheme 1). **FHQ-BR** and **FHQ-PB** have the same π -conjugated electronic structure with the main structural difference being the accompanying counterions for charge compensation of the terminal hexyltrimethylammonium groups. It is the same for **FPQ-BR** and **FPQ-PB**. A fluorescein (Fl)-labeled single-stranded DNA (ssDNA-Fl) was used as a FRET acceptor. The counterions are expected to remain close to the polymer chain and perturb the fine-structure of the electrostatic complex, CCP/ssDNA-Fl, e.g., the intermolecular D–A separation, which have a substantial effect on energy transfer and PCT (Scheme 1). As described in detail below, the same CCP backbones with different counterions behave differently as an excitation donor to ssDNA-Fl. This simple strategy for tuning the fine-structure

* Corresponding author. Telephone: 82-55-350-5300. Fax: 82-55-350-5653. E-mail: hywoo@pusan.ac.kr.

[†] Department of Nanofusion Technology (BK21), Pusan National University.

[‡] Department of Chemistry, Pusan National University.

Scheme 1. Molecular Structures of Cationic Polyfluorene Copolymers with Different Counterions and Their Complexation Schematics with ssDNA-FI

Scheme 2. Overall Synthetic Scheme ^a

^a Reagents and conditions: (i) $\text{Pd}(\text{PPh}_3)_4$, 2 M Na_2CO_3 , toluene, 80 °C, 24 h; (ii) trimethylamine in THF/methanol, room temperature, 48 h; (iii) excess ammonium tetraphenylborate in methanol, 48 h.

of the D/A complex on the molecular scale by exchanging counterions, suggests an easy and effective way for kinetic control of the fluorescence energy transfer for maximizing signal amplification in CPs-based FRET DNA detection. Moreover, this approach for signal enhancement is generally applicable to other conjugated polyelectrolytes, since the CPs have ionic end groups for water-solubility.

2. Experimental Section

General Information. All chemicals were purchased from Aldrich Chemical Co. and used as received unless otherwise mentioned. HPLC-purified single-stranded DNA labeled with fluorescein at the 5' position (ssDNA-FI) with 20 bases of the sequence (5'-FI-TTAA TCGA GTTA CCGC AATC-3') was obtained from Sigma-Genosys.

¹H NMR spectra were recorded on JEOL (JNM-AL300) FT NMR system. X-ray photoelectron spectrometer (XPS) data were measured at the Korea Basic Science Institute, Pusan National University. The XPS study was performed with a VG Scientific ESCALAB250 XPS system (U.K.) under a base pressure of 4×10^{-10} Torr (UHV), using monochromated Al K α X-ray source ($h\nu = 1486.6$ eV). Emitted photoelectrons were detected by a multi-channel detector at a take off angle of 90° relative to the sample surface. Survey spectra were obtained at a resolution of 1 eV, and high-resolution spectra were acquired at a resolution of 0.05 eV. The obtained binding energy (BE) was determined relative to the C1s core level peak at 284.6 eV as a reference. The number-average molecular weight of the polymers was determined by gel-permeation chromatography (GPC) on a Agilent Technologies 1200 Series. The UV/vis absorption spectra were measured with a Jasco (V-630)

spectrophotometer. The photoluminescence (PL) spectra were obtained on a Jasco (FP-6500) spectrofluorometer with a Xenon lamp excitation source, using 90 degree angle detection for solution samples. All FRET PL spectra were measured in 20 mM phosphate buffer unless otherwise stated. The fluorescence quantum yield was measured relative to a freshly prepared fluorescein in water at pH = 11.

Synthesis and Characterization of CCPs. Four different polyfluorene copolymers, **FHQ-BR** or **-PB** and **FPQ-BR** or **-PB** were synthesized using a modification of the procedures reported elsewhere.^{8,10,11} The neutral precursor polymer, **FHN**, was synthesized by Suzuki coupling 9,9-bis(6'-bromohexyl)fluorene diboric ester and 1,4-bis(6-bromohexyloxy)-2,5-dibromobenzene using $\text{Pd}(\text{PPh}_3)_4$ in toluene/ H_2O (2:1) under heating at 80 °C for 24 h. **FPN** was similarly obtained by a reaction between 2,7-dibromo-9,9-bis(6'-bromohexyl)fluorene and 1,4-phenylenebisboronic ester (Scheme 2). The degree of polymerization was determined to be $M_n = 15\,300$ g/mol (PDI = 2.03) for **FHN** and $M_n = 16\,700$ g/mol (PDI = 2.32) for **FPN** using GPC (solvent: THF) relative to a polystyrene standard. The water-soluble polymers, **FHQ-BR** and **FPQ-BR** were obtained by treating **FHN** and **FPN** with condensed trimethylamine at room temperature in a THF/methanol mixture for 48 h. **FHQ-PB** and **FPQ-PB** were prepared by counterion exchange reactions (repeated 3–4 times) by adding excess tetraphenylborate in methanol (~10 equiv). The extent of the counterions exchanged was determined by ¹H NMR and XPS measurements. In ¹H NMR spectra of **FHQ** (or **FPQ**)-**PB**, the new lines around 7 ppm are originated from the phenyl ring of **PB** and the peak integration indicates that bromides are replaced almost completely by the tetraphenylborate anions (Figure 1 and Supporting Information). In addition, Figure 2 also shows the Br(3d) signal of

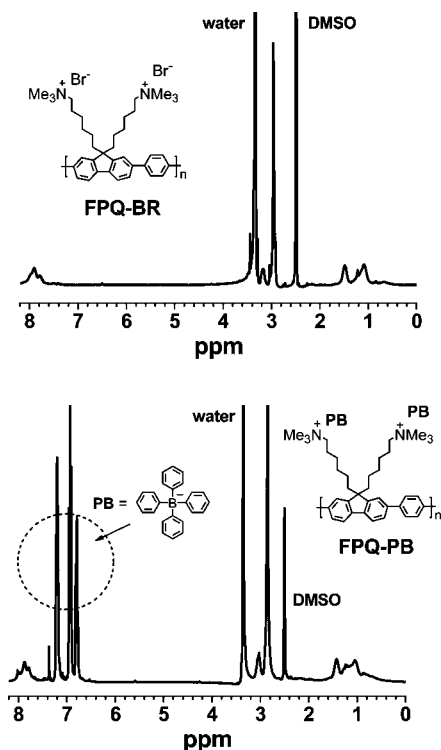


Figure 1. ^1H NMR (300 MHz, DMSO) spectra of **FPQ-BR** and **FPQ-PB**.

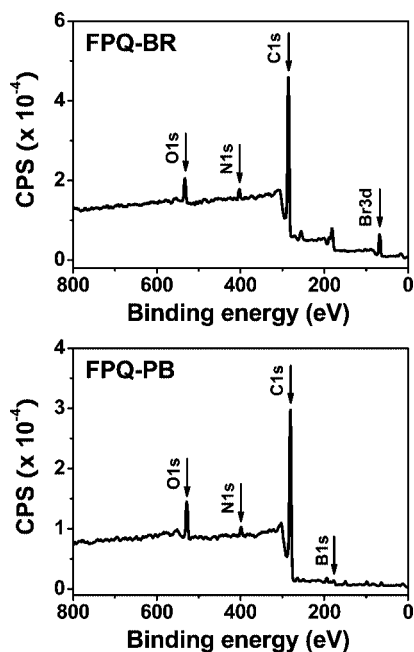


Figure 2. XPS spectra of **FPQ-BR** and **FPQ-PB**.

FPQ-BR around 64 eV disappears in the XPS spectrum of **FPQ-PB**. All the NMR and XPS data show good agreement with the proposed molecular structure of the polymers (Supporting Information). ^1H NMR (300 MHz, DMSO) δ (ppm), **FHQ-BR**: 8.0–7.10 (br, 8H), 4.06 (br, 4H), 3.30 (br, 8H), 3.10 (br, 18H), 3.02 (br, 18H), 1.80–0.70 (br, 36H). **FHQ-PB**: 8.0–7.45 (br, 6H), 7.31–7.17 (m, 34H), 6.92 (m, 32H), 6.83 (m, 16H), 4.00 (br, 4H), 3.10 (br, 8H), 2.94 (br, 18H), 2.79 (br, 18H), 1.90–0.90 (br, 36H). **FPQ-BR**: 8.10–7.60 (br, 10H), 3.17 (br, 4H), 2.96 (s, 18H), 1.6–0.9 (br, 20H). **FPQ-PB**: 8.10–7.60 (br, 10H), 7.17 (m, 16H), 6.90 (m, 16H), 6.77 (m, 8H), 3.04 (br, 4H), 2.83 (s, 18H), 1.6–0.8 (br, 20H).

3. Results and Discussion

UV/Vis and Photoluminescence Spectroscopic Properties. To examine the effect of counterions on the optical (and electronic) properties of the polymers, UV/vis and photoluminescence (PL) spectra were measured in DMSO in which both **FHQ-BR** and **FHQ-PB** are very soluble. The absorption and PL spectra of the two structures with different counterions overlapped exactly in DMSO ($\lambda_{\text{abs}} = 376$ nm, $\lambda_{\text{PL}} = 422$ nm, Figure 3). Two polymers also show similar PL quantum efficiency ($\Phi_{\text{PL}} = \sim 68\%$) in DMSO. This indicates that the counterions do not interact with the HOMO–LUMO electronic structure of the π -conjugated main backbone. As shown in Figure 3, the maxima in the absorption (λ_{abs}) and PL (λ_{PL}) for **FHQ-BR** in water were measured at 365 and 420 nm, which are similar to the values for **FHQ-PB** ($\lambda_{\text{abs}} = 365$ nm and $\lambda_{\text{PL}} = 426$ nm).¹² The slight difference might be related to the relatively poor solubility (and resulting conformational change and aggregation) of **FHQ-PB** in water. The same discussions are possible for **FPQ-BR** ($\lambda_{\text{abs}} = 381$ nm and $\lambda_{\text{PL}} = 423$ nm) and **FPQ-PB** ($\lambda_{\text{abs}} = 374$ nm and $\lambda_{\text{PL}} = 424$ nm) in water.

An estimation of the Connolly solvent-excluded volume (SEV) of the counterions (selecting water as a solvent probe), which is the volume of the space from which solvent is excluded by the presence of the molecule,¹³ indicates that the tetraphenylborate ion ($\text{SEV} = 314 \text{ \AA}^3$) is ca. 12 times larger than bromide ($\text{SEV} = 27 \text{ \AA}^3$). The polymers with **BR** and **PB** as a counterion have a similar electronic structure but different counterions which might alter the average interchain separation in the aggregated phases.¹¹ Previous studies also reported the counterion effect on the conformation¹⁴ or morphology¹⁵ of the polymers. The effect of the counterions on the electrostatic complexation was examined by measuring λ_{abs} of FI before and after complexation with excess CCPs ($[\text{CCP}] = \sim 2 \times 10^{-5} \text{ M}$, $[\text{ssDNA-FI}] = 8 \times 10^{-7} \text{ M}$). The absorption maximum of ssDNA-FI in the absence of the polymers was measured at 494.5 nm. After complexation with CCPs, λ_{abs} of FI is red-shifted to 509.1 nm ($\Delta\lambda_{\text{abs}} = 14.6$ nm) for **FHQ-BR**/ssDNA-FI, 496.3 nm ($\Delta\lambda_{\text{abs}} = 1.8$ nm) for **FHQ-PB**/ssDNA-FI, 506.6 nm ($\Delta\lambda_{\text{abs}} = 12.1$ nm) for **FPQ-BR**/ssDNA-FI and 497.1 nm ($\Delta\lambda_{\text{abs}} = 2.6$ nm) for **FPQ-PB**/ssDNA-FI. This absorption shift is related to a change in the local environment around FI due to the complexation with the polymers. The polymers with **BR** induce much larger red-shift in λ_{abs} of ssDNA-FI with compared to **PB** exchanged polymers, indicating the tighter complexation with ssDNA-FI. This reflects that the counterions can perturb the electrostatic complexation of the polymers with ssDNA-FI. It is expected the weaker binding between the optically active D (CCP) and A (ssDNA-FI) units, and the longer D–A intermolecular separation for the polymers with the larger counterion (**PB**).

FRET-Induced PL Spectroscopy. To examine how the accompanied counterions influence the PL energy transfer to ssDNA-FI, we investigated the FRET-induced emission characteristics. Fluorescein was chosen as a FRET acceptor due to good spectral overlap with the polymers (λ_{PL} (CCP) = ~ 420 nm and λ_{abs} (FI) = 494.5 nm). The opposite charges on the polymer backbone and oligonucleotide allow the formation of an electrostatic complex, CCP/ssDNA-FI, enabling facile energy transfer from CCPs to ssDNA-FI. The measurements were carried out in an aqueous phosphate buffer (20 mM, pH = 8.1) containing $[\text{ssDNA-FI}] = 2.5 \times 10^{-8} \text{ M}$ with increasing CCP concentration ($[\text{FHQ-BR}] = [\text{FHQ-PB}] = 0 \sim 5.9 \times 10^{-7} \text{ M}$ and $[\text{FPQ-BR}] = [\text{FPQ-PB}] = 0 \sim 1.2 \times 10^{-6} \text{ M}$ based on the polymer repeating units (RUs)). The final concentration of the polymers corresponds to a charge ratio of 4.8:1 ([+] in CCP: [–] in ssDNA-FI).

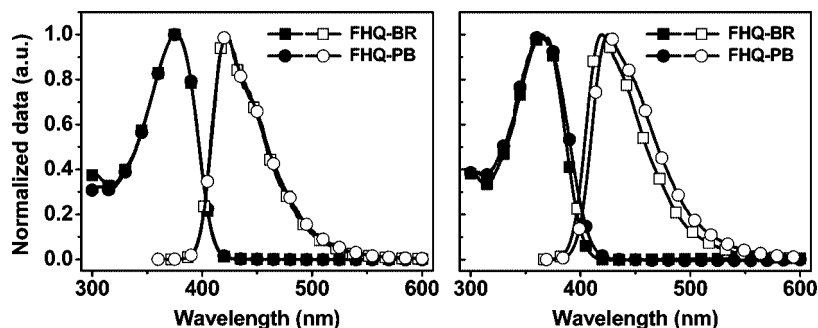


Figure 3. Absorption (filled) and emission (open) spectra of **FHQ**s in DMSO (left) and water (right).

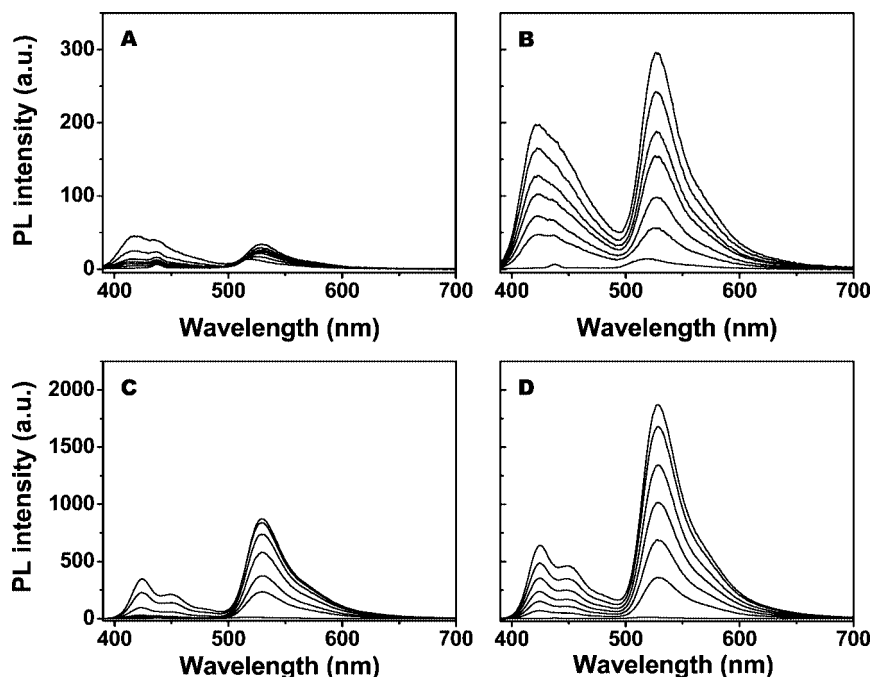


Figure 4. FRET-induced PL spectra of (a) **FHQ-BR**/ssDNA-FI, (b) **FHQ-PB**/ssDNA-FI, (c) **FPQ-BR**/ssDNA-FI and (d) **FPQ-PB**/ssDNA-FI with increasing [CCP] by exciting at 380 nm. [ssDNA-FI] = 2.5×10^{-8} M, [**FHQ-BR**] = [**FHQ-PB**] = $0-5.9 \times 10^{-7}$ M, [**FPQ-BR**] = [**FPQ-PB**] = $0-1.2 \times 10^{-6}$ M.

Figure 4 shows the FRET-induced FI emission spectra in **FHQ**/ssDNA-FI and in **FPQ**/ssDNA-FI upon excitation of the polymers at 380 nm. It should be noted that all spectra were not normalized and were measured under the same conditions. Almost complete PL quenching of both the polymer ($\lambda_{PL} \sim 420$ nm) and FI ($\lambda_{PL} \sim 530$ nm) was observed in the case of **FHQ-BR**/ssDNA-FI (Figure 4a). The same observation has been reported in the literatures,^{6,10} in which serious PL quenching with a negligible FRET signal was interpreted in terms of photoinduced charge transfer as a possible mechanism. PCT is thermodynamically favorable from **FHQ-BR** to FI due to the electronic structures of the D/A pairs (HOMO (−5.6 eV) and LUMO (−2.5 eV) for **FHQ-BR**, HOMO (−5.8 eV) and LUMO (−3.4 eV) for FI). However, a clear FRET FI signal and the polymer emission were recovered in the electrostatic **FHQ-PB**/ssDNA-FI complex with the bulkier tetraphenylborate as shown in Figure 4b. The final FRET FI emission is ~ 8.6 times higher than that of **FHQ-BR**/ssDNA-FI. Similar observations were measured in **FPQ**/ssDNA-FI, in which the polymer with larger **PB** induces twice the enhanced FRET FI signal relative to **FPQ-BR**. We also measured a clear trend in the counterion effects with a series of **FPQ** polymers with additional counterions: tetrafluoroborate (**FB**, SEV = 52 \AA^3), hexafluorophosphate (**FP**, SEV = 79 \AA^3) and tetrakis(1-imidazolyl)borate (**IB**, SEV = 278 \AA^3). The PL intensity of the FRET-induced FI

signal is gradually increased with increasing the size of the counterions (Supporting Information). The bulkier counterions such as **IB** and **PB** induce more enhanced FRET signal amplification as compared with the smaller counterions (**BR**, **FB** and **FP**).

As mentioned above, the larger counterion induces weaker complexation with increasing D–A intermolecular separation, in turn which may reduce FRET efficiency from the polymers to ssDNA-FI. Figure 5 displays the FRET ratio ($I_{\text{FRET-FI}}/I_{\text{CCP}}$) data for the complexes CCP/ssDNA-FI, as a function of charge ratio ([+]:[−] in CCP: [−] in ssDNA-FI). It is calculated by taking the PL intensity ratio of FRET-induced FI emission (at ~ 530 nm) over the residual CCP emission (at ~ 420 nm) at each peak wavelength. The FRET ratio is closely related to the FRET efficiency. At the charge ratio of 0.8:1 ([+]:[−]), all the polymers are expected to form the complex with ssDNA-FI. As the charge ratio is increased with increasing [CCP], the FRET ratio will be decreased due to the emission from the uncomplexed free polymers which do not contribute to the FRET signal and just enhance the polymer emission. The FRET ratio at 0.8:1 charge ratio was determined to be 18.6 for **FPQ-BR**/ssDNA-FI, 5.0 for **FPQ-PB**/ssDNA-FI, and ~ 1.2 for **FHQ-PB**/ssDNA-FI, respectively ([**FPQ-BR**] = [**FPQ-PB**] = 2×10^{-7} M, [**FHQ-PB**] = 1×10^{-7} M and [ssDNA-FI] = 2.5×10^{-8} M). Unfortunately we could not measure the exact FRET ratio for

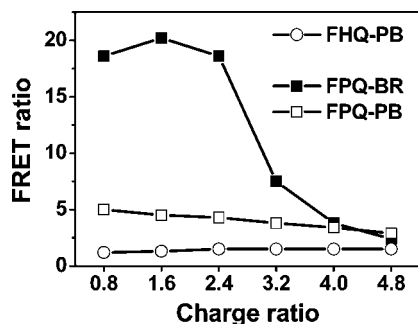


Figure 5. FRET ratio ($I_{\text{FRET-FI}}/I_{\text{CCP}}$) as a function of charge ratio ($[+]$ in CCP/ $[−]$ in ssDNA-FI).

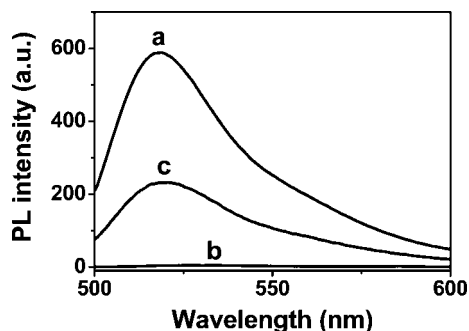


Figure 6. PL spectra of ssDNA-FI in the absence of the polymers (a) and in the presence of excess polymers, **FHQ-BR** (b) and **FHQ-PB** (c), upon direct excitation of FI at 490 nm. $[\text{ssDNA-FI}] = 2.5 \times 10^{-8}$ M, $[\text{FHQ-BR}]$ or $[\text{FHQ-PB}] = 5.9 \times 10^{-7}$ M.

FHQ-BR/ssDNA-FI due to the serious PL quenching for both the polymer and FI. For the polymers with **PB**, much lower FRET ratio was measured relative to the polymers with **BR**. The lower FRET ratio with **PB** can be explained by the increased D–A intermolecular separation due to the existence of the larger counterions in between the polymer and DNA. Interestingly the FRET ratio (or efficiency) was decreased but the FRET-induced FI emission was amplified by the polymers with the bulkier **PB** (see Figure 4).

FI Emission upon Direct Excitation. Additional important information concerning the effect of counterions was obtained from the FI emission measurements after complexation by directly exciting FI at 490 nm. The measurements were carried out in the presence of excess polymers ($[\text{ssDNA-FI}] = 2.5 \times 10^{-8}$ M, $[\text{FHQ}] = 5.9 \times 10^{-7}$ M, $[+]$ in CCP: $[−]$ in ssDNA-FI = 4.8:1), in which the amount of uncomplexed free ssDNA-FI is expected to be negligible. As shown in Figure 6, ssDNA-FI is highly emissive ($\Phi_{\text{PL}} \sim 80\%$) in the absence of the polymers but FI emission is almost completely quenched after complexation in **FHQ-BR**/ssDNA-FI. The PL quenching via the electron (or charge) transfer from the polymer to HOMO of the excited FI* was suggested in the previous literatures.^{6,10,16} The FRET-induced FI signal cannot be expected if the charge transfer occurs within the lifetime of the excited FI*. The PL lifetime of FI* was reported to be ~ 4 ns and the charge transfer occurs within the pico- or femto-second time scale.¹⁶ We measured clear decrease in PL lifetime of the excited FI* (in ssDNA-FI) via PCT quenching in the presence of **FHQ-BR** (PL lifetime of FI: 4 ns \rightarrow 78 ps).^{16b} Relatively moderate quenching of FI was observed in the case of **FHQ-PB**/ssDNA-FI, where FI* is still highly emissive after forming an electrostatic complex. For **FPQ** with **BR** and **PB**, the larger counterion also induces much lower PL quenching of FI* in the presence of excess polymers. In addition, the concentration self-quenching of FI in the complex was suggested as another possible mechanism.⁸ As compared to **FHQ-BR**, the complexation of

FHQ-PB and ssDNA-FI is expected to be less tight and as a consequence, the overall volume of **FHQ-PB**/ssDNA-FI be larger and the resulting DNA compaction within the complex must be attenuated. Accordingly, the concentration self-quenching of FI can be reduced in **FHQ-PB**/ssDNA-FI complex. The PL quenching should be minimized in order to increase the FRET-induced emission which is closely related to the detection sensitivity in CPs-based FRET DNA sensors.

The above observation can be understood in terms of the enhanced FI emission at the expense of the PCT process due to the increased D–A intermolecular distance by the loose complexation in CCP/ssDNA-FI with bulkier tetraphenylborate. Both **FHQ-BR** and **FHQ-PB** (or **FPQ-BR** and **FPQ-PB**) have the same HOMO–LUMO electronic structure with the same thermodynamic driving forces for PCT. The counterions accompanying the polymer chain may perturb the complexation and modify the fine-structure of D/A electrostatic complex, i.e., D–A intermolecular separation, which kinetically reduces the rate of PCT process. It is believed that the hydrophobicity as well as physical size of the counterions influences the formation and fine-structure of the CCP/ssDNA-FI complex.

Overall quenching effects on ssDNA-FI by the presence of polymers were quantified by using Stern–Volmer (SV) equation

$$\frac{I_0}{I} = 1 + K_{\text{SV}}[Q] \quad (1)$$

where I and I_0 are the PL intensity of ssDNA-FI in the presence and absence of the polymers and $[Q]$ is the concentration of the polymers (quencher). Measurements were carried out in the solution of $[\text{ssDNA-FI}] = 2.5 \times 10^{-8}$ M in 20 mM phosphate buffer, by increasing $[\text{FHQ-BR}] = [\text{FHQ-PB}] = 2.5 \times 10^{-8}$ M to 1.74×10^{-7} M and $[\text{FPQ-BR}] = [\text{FPQ-PB}] = 5.0 \times 10^{-8}$ M to 3.5×10^{-7} M. The Stern–Volmer quenching constant, K_{SV} was calculated employing the linear region of Stern–Volmer plot (I_0/I vs $[Q]$, Figure 7). The K_{SV} values for ssDNA-FI complexed with **FHQ-BR**, **FHQ-PB**, **FPQ-BR** and **FPQ-PB** were calculated to be $4.3 \times 10^6 \text{ M}^{-1}$, $2.2 \times 10^6 \text{ M}^{-1}$, $2.8 \times 10^6 \text{ M}^{-1}$ and $1.3 \times 10^6 \text{ M}^{-1}$, respectively. By considering the PL lifetime of FI ($\tau_{\text{FI}} = \sim 4$ ns), the quenching rate ($k_q = K_{\text{SV}}/\tau_{\text{FI}}$) of ssDNA-FI by complexation with CCPs was determined to be $1.0 \times 10^{15} \text{ M}^{-1} \text{ s}^{-1}$ for **FHQ-BR**/ssDNA-FI, $5.2 \times 10^{14} \text{ M}^{-1} \text{ s}^{-1}$ for **FHQ-PB**/ssDNA-FI, $6.7 \times 10^{14} \text{ M}^{-1} \text{ s}^{-1}$ for **FPQ-BR**/ssDNA-FI and $3.1 \times 10^{14} \text{ M}^{-1} \text{ s}^{-1}$ for **FPQ-PB**/ssDNA-FI, respectively. The magnitude of k_q which is $\sim 10^4$ times larger than the up-limit of dynamic quenching rate ($10^{10} \text{ M}^{-1} \text{ s}^{-1}$) implies the quenching mechanism of FI in the CCP/ssDNA-FI complex is mainly contributed by static quenching caused by the formation of nonradiative complex with CCPs.¹⁷ The k_q values of ssDNA-FI complexed with **FHQ-PB** and **FPQ-PB** are smaller than those with **FHQ-BR** and **FPQ-BR**, confirming much reduced (by half) PL quenching of FI by the polymers with larger counterions.

PL Quantum Efficiency of FRET-Induced FI Signal. The PL quantum efficiency ($\Phi_{\text{FRET-PL}}$) of the FRET-induced FI signal was measured to obtain insight into the energy transfer process by using the polymers with different counterions. For the quantum efficiency measurements, a more concentrated condition ($[\text{ssDNA-FI}] = 8 \times 10^{-7}$ M, $[\text{FHQ-BR}] = [\text{FHQ-PB}] = 2.0 \times 10^{-6}$ M, $[\text{FPQ-BR}] = [\text{FPQ-PB}] = 4.0 \times 10^{-6}$ M) is necessary to measure the exact absorption, in which similar FRET data were observed with respect to those in the diluted condition. The 0.5:1 ($[+]$ in CCP: $[−]$ in ssDNA-FI) charge ratio was chosen in order to minimize the uncomplexed free polymers which do not contribute to the FRET signal. The FRET PL efficiency in the CCP/ssDNA-FI complex was determined by exciting the polymer and

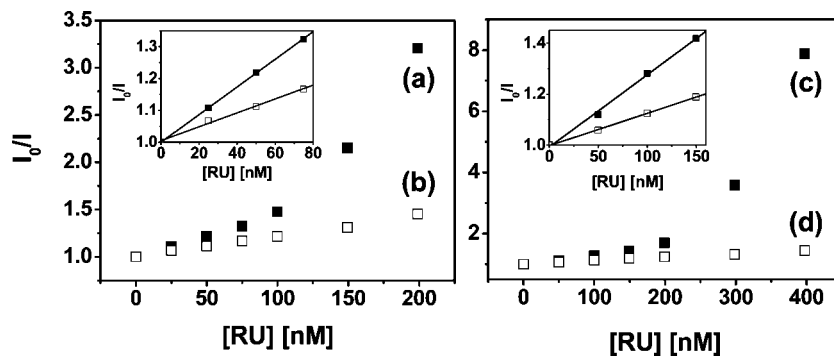


Figure 7. Stern–Volmer plot of ssDNA-FI with increasing polymer concentration, **FHQ-BR** (a) **FHQ-PB** (b), **FPQ-BR** (c) and **FPQ-PB** (d). (Inset: linear region of Stern–Volmer plot.)

measuring the FRET FI signal, relative to fluorescein in water at pH = 11. The measured $\Phi_{\text{FRET-PL}}$ is 8.7 for **FPQ-BR**/ssDNA-FI and 16.5 for **FPQ-PB**/ssDNA-FI, respectively. The $\Phi_{\text{FRET-PL}}$ for **FHQ-BR**/ssDNA-FI is negligible ($\sim 1\%$) but **FHQ-PB** shows much improved $\Phi_{\text{FRET-PL}}$ of 10.9. The polymers with the larger **PB** induce much improved PL quantum efficiency of the FRET-induced FI signal.

By combining the above PL data (by exciting the polymer and FI), it appears that the PCT decreased more substantially relative to FRET with changing bromide to tetraphenylborate as a counterion. Both FRET and PCT are very sensitive to the D–A intermolecular distance ($r_{\text{D-A}}$). The PCT rate (k_{PCT}) shows an exponential decrease with increasing $r_{\text{D-A}}$ while the FRET rate (k_{FRET}) is proportional to $r_{\text{D-A}}^{-6}$. The improved $\Phi_{\text{FRET-PL}}$ in **FHQ-PB** (or **FPQ-PB**)/ssDNA-FI is interpreted in terms of the more substantial decrease of the acceptor quenching due to the loose complexation with the increased D–A separation, even though the FRET efficiency was decreased. This suggests that the competition between thermodynamically favorable PCT and FRET can be controlled kinetically by modulating the D/A fine-structure on the molecular scale using different counterions.

4. Conclusion

In summary, two conjugated polyelectrolytes (**FHQ**, **FPQ**) with two different counterions (bromide or tetraphenylborate) were studied as a FRET donor to a fluorescein-labeled oligonucleotide (ssDNA-FI). The polymers with different counterions have the same π -conjugated electronic structure, and the accompanied counterions might perturb the intermolecular separation with ssDNA-FI in the electrostatic complex. The FRET FI signal was enhanced 2–8.6 times by changing bromide to tetraphenylborate as a counterion by virtue of the weaker complexation between the optically active D and A units, the larger D–A separation and the reduced photoinduced charge transfer quenching. Although the precise fine-structure of the CCP/ssDNA-FI complex is poorly understood at present stage, these findings suggest an simple strategy to tune the fine-structure of the electrostatic complex, e.g., the D–A intermolecular distance on the molecular scale. Larger counterions induce weaker complexation with ssDNA-FI and decrease the rate of both FRET and PCT, but the competition between them was successfully controlled using counterions with different sizes. This simple strategy provides an important idea how to minimize the thermodynamically favorable PCT for maximizing the signal amplification in CPs-based FRET DNA detection. A more detailed study on the counterion effect is currently underway using time-resolved PL spectroscopy to obtain insight into the fine-structure of the D/A complex.

Acknowledgment. This work was supported by the Korea Research Foundation Grant funded by the Korean Government

(MOEHRD, KRF-2006-331-D00139) and International Cooperation Research Program of the Ministry of Science & Technology, Korea (M6-0605-00-0005).

Supporting Information Available: Text giving synthetic details and figures showing additional ^1H NMR, XPS, UV–vis, PL spectra of the polymers and the FRET-induced PL spectra in the presence of additional counterions. This material is available free of charge via the Internet at <http://pubs.acs.org>.

References and Notes

- (1) (a) Nilsson, K. P. R.; Inganäs, O. *Nat. Mater.* **2003**, *2*, 419. (b) Pinto, M. R.; Schanze, K. S. *Proc. Natl. Acad. Sci. U.S.A.* **2004**, *101*, 7505. (c) Kumaraswamy, S.; Bergstedt, T.; Shi, X.; Rininsland, F.; Kushon, S.; Xia, W.; Ley, K.; Achyuthan, K.; McBranch, D.; Whitten, D. *Proc. Natl. Acad. Sci. U.S.A.* **2004**, *101*, 7511.
- (2) (a) Zhao, D.; Du, J.; Chen, Y.; Ji, X.; He, Z.; Chan, W. *Macromolecules* **2008**, *41*, 5373. (b) McQuade, D. T.; Pullen, A. E.; Swager, T. M. *Chem. Rev.* **2000**, *100*, 2537. (c) Liu, B.; Bazan, G. C. *Chem. Mater.* **2004**, *16*, 4467. (d) Zheng, J.; Swager, T. M. *Macromolecules* **2006**, *39*, 6781.
- (3) (a) Lee, S. W.; Sanedrin, R. G.; Oh, B.-K.; Mirkin, C. A. *Adv. Mater.* **2005**, *17*, 2749. (b) Song, J.; Cisar, J. S.; Bertozzi, C. R. *J. Am. Chem. Soc.* **2004**, *126*, 8459. (c) He, F.; Tang, Y.; Yu, M.; Wang, S.; Li, Y.; Zhu, D. *Adv. Funct. Mater.* **2006**, *16*, 91. (d) Feng, F.; Tang, Y.; Wang, S.; Li, Y.; Zhu, D. *Angew. Chem., Int. Ed.* **2007**, *46*, 7882. (e) Ambade, A. V.; Sandanaraj, B. S.; Klaukherd, A.; Thayumanavan, S. *Polym. Int.* **2007**, *56*, 474. (f) Thomas III, S. W.; Joly, G. D.; Swager, T. M. *Chem. Rev.* **2007**, *107*, 1339. (g) Xing, C.; Yu, M.; Wang, S.; Shi, Z.; Li, Y.; Zhu, D. *Macromol. Rapid Commun.* **2007**, *28*, 241.
- (4) Ho, H.-A.; Boissinot, M.; Bergeron, M. G.; Corbeil, G.; Doré, K.; Boudreau, D.; Leclerc, M. *Angew. Chem., Int. Ed.* **2002**, *41*, 1548.
- (5) (a) Li, H.; Yang, R.; Bazan, G. C. *Macromolecules* **2008**, *41*, 1531. (b) Gaylord, B. S.; Heeger, A. J.; Bazan, G. C. *Proc. Natl. Acad. Sci. U.S.A.* **2002**, *99*, 10954. (c) Gaylord, B. S.; Heeger, A. J.; Bazan, G. C. *J. Am. Chem. Soc.* **2003**, *125*, 896. (d) Pu, K.-Y.; Fang, Z.; Liu, B. *Adv. Funct. Mater.* **2008**, *18*, 1321. (e) Ho, H. A.; Doré, K.; Boissinot, M.; Bergeron, M. G.; Tanguay, R. M.; Boudreau, D.; Leclerc, M. *J. Am. Chem. Soc.* **2005**, *127*, 12673. (f) Peng, H.; Soeller, C.; Travas-Sejdic, J. *Chem. Commun.* **2006**, 3735. (g) He, F.; Feng, F.; Duan, X.; Wang, S.; Li, Y.; Zhu, D. *Anal. Chem.* **2008**, *80*, 2239. (h) Duan, X.; Li, Z.; He, F.; Wang, S. *J. Am. Chem. Soc.* **2007**, *129*, 4154. (i) Tian, N.; Tang, Y.; Xu, Q.-H.; Wang, S. *Macromol. Rapid Commun.* **2007**, *28*, 729. (j) Lv, W.; Li, N.; Li, Y.; Li, Y.; Xia, A. *J. Am. Chem. Soc.* **2006**, *128*, 10281. (k) Lee, K.; Povlich, L. K.; Kim, J. *Adv. Funct. Mater.* **2007**, *17*, 2580. (l) Lee, K.; Rouillard, J.-M.; Pham, T.; Gulari, E.; Kim, J. *Angew. Chem.* **2007**, *119*, 4751.
- (6) Woo, H. Y.; Vak, D.; Korystov, D.; Mikhailovsky, A.; Bazan, G. C.; Kim, D.-Y. *Adv. Funct. Mater.* **2007**, *17*, 290.
- (7) Liu, B.; Gaylord, B. S.; Wang, S.; Bazan, G. C. *J. Am. Chem. Soc.* **2003**, *125*, 6705.
- (8) (a) Wang, S.; Bazan, G. C. *Chem. Commun.* **2004**, 2508. (b) Liu, B.; Bazan, G. C. *Chem. Asian J.* **2007**, *2*, 499.
- (9) (a) Heeger, P. S.; Heeger, A. J. *Proc. Natl. Acad. Sci. U.S.A.* **1999**, *96*, 12219. (b) Xu, Q.-H.; Gaylord, B. S.; Wang, S.; Bazan, G. C.; Moses, D.; Heeger, A. J. *Proc. Natl. Acad. Sci. U.S.A.* **2004**, *101*, 11634.
- (10) Liu, B.; Bazan, G. C. *J. Am. Chem. Soc.* **2006**, *128*, 1188.
- (11) Yang, R.; Garcia, A.; Korystov, D.; Mikhailovsky, A.; Bazan, G. C.; Nguyen, T.-Q. *J. Am. Chem. Soc.* **2006**, *128*, 16532.

- (12) The aqueous polymer solution was prepared by dilution by 100–1000 times of each polymer stock solution in DMSO (10^{-3} M or 10^{-4} M).
- (13) Connolly, M. L. *J. Am. Chem. Soc.* **1985**, *107*, 1118.
- (14) McCullough, R. D.; Ewbank, P. C.; Loewe, R. S. *J. Am. Chem. Soc.* **1997**, *119*, 633.
- (15) Yang, R.; Wu, H.; Cao, Y.; Bazan, G. C. *J. Am. Chem. Soc.* **2006**, *128*, 14422.
- (16) (a) Götz, M.; Hess, S.; Beste, G.; Skerra, A.; Michel-Beyerle, M. E. *Biochemistry* **2002**, *41*, 4156. (b) Nayak, R. R.; Nag, O. K.; Woo, H. Y.; Hwang, S.; Vak, D.; Korystov, D.; Jin, Y.; Suh, H. *Curr. Appl. Phys.* **2008**, in press (doi: 10.1016).
- (17) Pu, K.-Y.; Pan, S. Y.-H.; Liu, B. *J. Phys. Chem. B* **2008**, *112*, 9295.

MA802647U